Double Sided LGAD Design Studies

FERMILAB-FN-1139-CMS-PPD

R. Lipton
Fermilab, Batavia, USA

January 2021

Abstract

We summarize TCAD design studies for double sided thick buried layer Low Gain Avalanche Diodes (LGADs). These thick double sided devices introduce new features that require overall optimization. We describe both the parameterized and full process simulation and discuss how the results affect the range of process and LGAD physical parameters.

1 Introduction

The double sided Low Gain Avalanche Diode (LGAD) is a variant of the pad-based LGADs that have been intensively studied over the last several years [1] [2] [3] [] and are now featured in timing layers for the ATLAS and CMS HL-LHC upgrade programs [4] [5]. The LGADs used for these projects utilize thin (typically about 50 micron) drift regions with a high energy "reach through" implant to define the gain layer which defines the high field amplification region. In previous work we have designed and prototyped an alternate gain structure, which utilizes a "buried" layer implanted before an epitaxial gain region is deposited. This alternate structure provides flexibility in design and importantly, allows for a gain layer of arbitrary depth. It is expected that a deeper layer will be more radiation hard than the standard reach-through device [6].

In this work we add a segmented strip or pixel array to the p-side of the LGAD with thicker bulk. This allows for double-sided readout with top side reading out the slower-drifting holes. For a device with the bulk thickness large compared to the pixel pitch the p-side readout can function as a mini time projection chamber with the drift time providing information on the depth of origin of the charge cloud. The signal p-side has two components, holes from the primary ionization followed by the larger number of holes generated at the gain layer. This provides a unique signature of the pattern of charge deposit within the device (figure 1). The overall features of the DS-LGAD are described in [7].

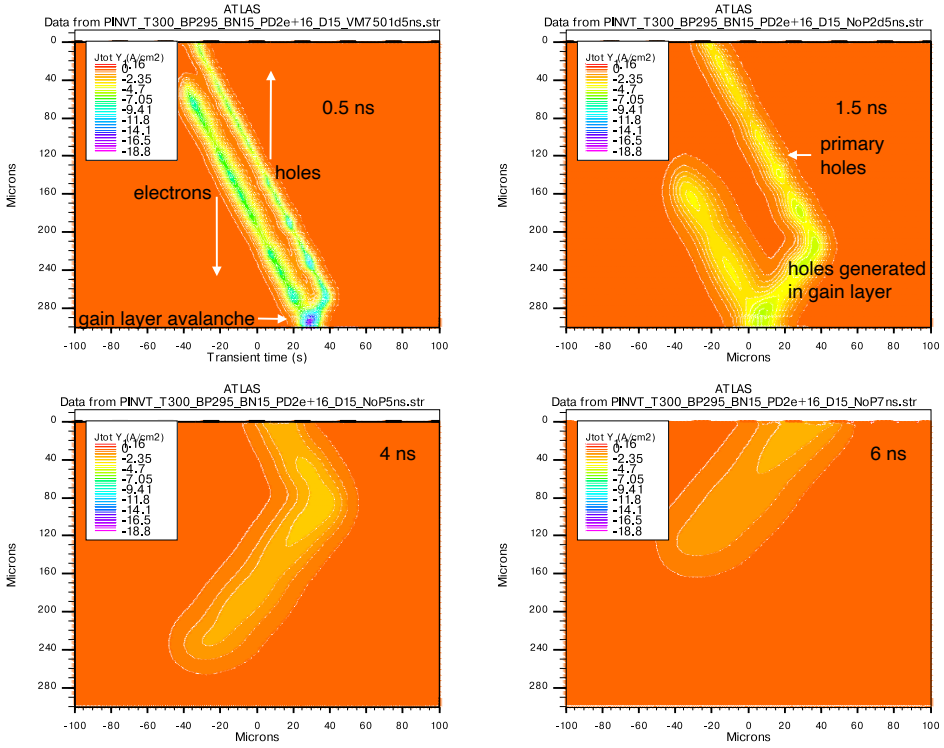

Figure 1: Snapshots of summed vertical electron and hole currents in a 300 micron thick double sided LGAD at various times after the initial charge deposition.

2 Features of the DS LGAD

Operation of the thick LGAD is sensitive to the interplay between the device thickness, gain layer location and doping, and the applied field. Avalanche multiplication begins at a field of about $3.2 \times 10^5 V/cm$ and rises rapidly until it saturates below $3.5 \times 10^5 V/cm$. We need gain fields in this range to achieve successful controlled gain. A significant field also needs to penetrate into the drift region which constitutes the bulk of the detector to insure sufficiently fast hole drift.

The structure of the simulated double sided LGAD is shown in figure 2a. In operation a positive bias is applied to the n+ (bottom) electrode. As the bias is raised the field increases in the region between the n+ bottom electrode and the p-type gain implant. The field increase is rapid since effective gap between the $n+/p_{gain}$ implants is small $dE/\,dV \approx 1/d_{gap}$. The rapid increase continues until the gain implant is fully depleted. This leaves a layer of positive charge that terminates the majority of the field lines. Additional bias voltage then will

deplete the bulk of the LGAD generating the drift field outside the gain region. When the LGAD is fully depleted the field increases as $1/thickness$; much more slowly in a thick device than in a thin one. This is demonstrated in figure 2b comparing the mid-gain and mid-drift region fields as a function of bias voltage for 50 and 300 micron thick LGADs. This means that while it is more difficult to attain high drift velocities in a thick LGAD the device can operate over a much wider voltage range since $dE/\,dV$ in the gain region after depletion is small.

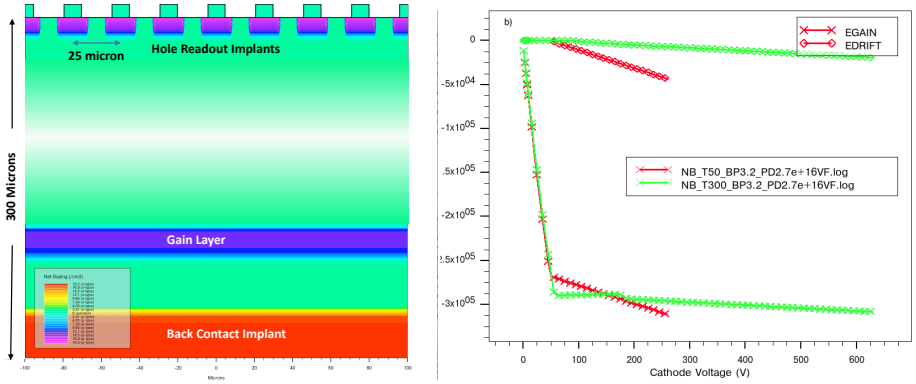

Figure 2: a) Sketch of the structure of the double sided LGAD as modeled. The width of the gain layer in all simulations is about 1 micron. Doping and depth of the gain layer are varied. b) Electric fields as a function of bias voltage at the middle of the gain layer (crosses) and at the middle of the device (diamonds) for devices with 50 micron (red) and 100 micron thickness.

3 Parameterized Design

Desirable characteristics of the LGAD include:

- Moderate operating voltage
- Large operating voltage range
- Heavily doped gain layer
- Deep gain layer
- Stable gain

A goal of these studies is to optimize operational characteristics and radiation resistance. The acceptor removal effect is the dominant source of loss of gain during LGAD irradiation is minimized by heavy gain layer doping. However

there is a trade-off between the depth of the gain layer and it's doping. A heavily doped gain layer will typically need to be shallow and have a short operating voltage window. A deep gain layer will have a lower field at a given bias voltage but a longer path for charge multiplication. It has been suggested that for irradiated sensors the longer gain path provides a longer lifetime than a shallower, more highly doped junction [**?**]. We study the tradeoff between gain layer depth and doping in a thick LGAD using a Silvaco [] TCAD model.

The model is shown in figure 2a. The gain layer is modeled as an $\approx 1\mu m$ thick layer doped as a flat $0.5\mu m$ core and a gaussian falloff. We record the fields in the gain and drift region as well as the impact generation rate in the gain region as a function of bias voltage. The gain layer depth is varied between 2.5 and 3.2 μm. At each step in the simulation the maximum ionization integral (II) from the n+ contact is recorded. The ionization integral is then used to estimate the gain as $\frac{1}{(1-II)}$. This gives a rough estimate of the gain, but is limited to gains below ≈ 20 due to the step size of the simulation, which must be small near ionization integral values close to 1.

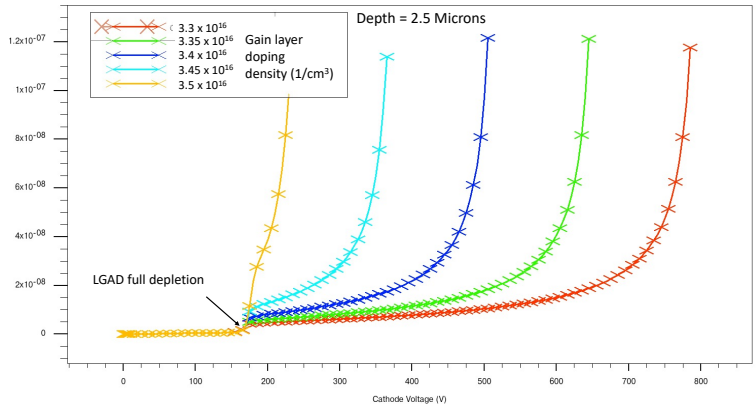

Figure 3: Cathode current as a function of bias voltage.

Figure 3 shows the current as a function of bias for LGADs with $2.5mum$ gain layer depth. Breakdown voltage decreases with doping density at the expense of operating voltage range. Additional doping beyond 3.5×10^{16} steepens the VI curve near the 180V break. Figure 7 shows corresponding ionization integrals and gain distributions for and LGAD with $3.2\mu m$ gain layer depth. The field in the gain region and the corresponding ionization integral increases rapidly until the gain layer is depleted at about 60V. The field then extends into the bulk and the ionization integral remains roughly constant (or falls a bit?). The gain at bias voltages between gain layer and device depletion (figure 7b) saturates at values below 10 until the gain region field again increases after full depletion of the device near 180V.

Figure 5 summarizes voltage to reach a gain of ≈ 20 as a function of gain layer peak doping for three values of the gain layer depth. In general the limit-

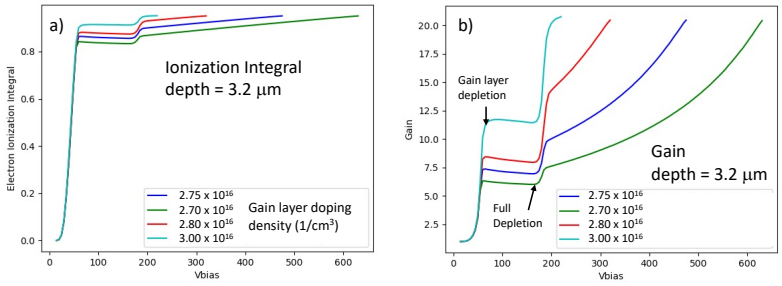

Figure 4: a) Impact ionization and b) gain as a function of bias voltage for a simulated LGAD with a gain layer depth of 3.2 μm

ing voltage (and the operating range) of the device decreases linearly with the peak doping. All curves converge to a limiting value of $\approx 200V$ at high doping values. Points with higher doping are included in the $3.2\mu m$ data as an example of this trend. The relation between required doping and gain layer depth means that these two effects have to be simultaneously optimized to achieve good performance and radiation hardness. As a reminder a deeper implant is considered more radiation hard but, as is shown in figure 5, a deep implant requires lower doping which is more sensitive to radiation-induced acceptor removal. Optimization of these parameters requires both a realistic radiation simulation and radiation testing of candidate devices.

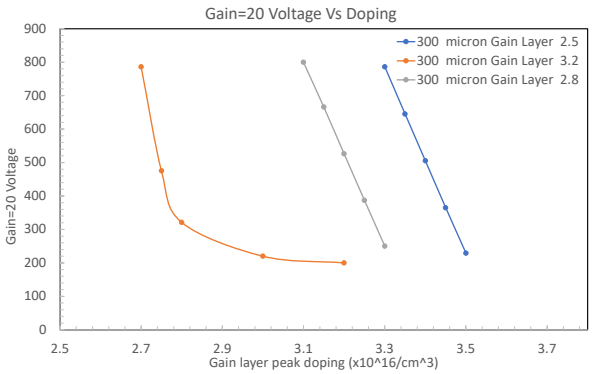

Figure 5: Curves of the gain = 20 bias voltage as a function of gain layer peak doping for constant values of the gain layer depth.

4 Process Flow

The simulation discussed in section 3 was based on the parameterization of a final device. To get a more realistic model we need to simulate the full process flow. This will give us a more accurate model of the doping profile. The doping profile of the gain layer and the resulting doping density directly affects the acceptor removal rate and thus radiation hardness. This is in turn affected by the thermal processing used in epitaxy and annealing processes. In these studies we use an epitaxial thickness of 2.8 microns and vary the gain layer doping and substrate thickness.

4.1 Process Steps

The process flow is modeled in the Silvaco Athena package. Simulator commands are prefixed by dashes. Variables, indicated by "+" are included in the control file to vary bulk material, implant energies, epitaxy thickness and annealing temperatures. he simulation includes the following steps:

1. Define the bulk material and resistivity - init silicon +Cty=+Dbulk orientation=100 two.d
2. etch oxide all - remove initial oxydation (RL)
3. gain layer pattern
4. gain layer implant - implant boron dose=+BLD energy=+BIEnergy amorph pearson tilt=7 rotation=0
5. Etch resist and oxide - etch photoresist all
6. anneal before epi deposit - diffus time=+tepia minutes temp=800 nitro
7. epi layer deposition - epitaxy time=56 minutes temp=900 thickness=2.8 dy=0.2 +Cty=2e12
8. p-spray implant - implant boron dose=1E12 energy=25 amorph pearson tilt=7 rotation=0
9. n+ top implant
10. top protection - deposit oxide thick=0.3
11. Flip Wafer - structure flip.y
12. Pattern p-side p+ implant
13. Implant p-side - implant boron dose=5e14 energy=40 crystal pearson tilt=0 rotation=0
14. remove photoresist - etch photoresist all
15. anneal all implants - diffus time=+tanneal minutes temp=800 nitro
16. Deposit bottom oxide - deposit oxide thick=.3
17. etch bottom side contact holes
18. flip to wafer top - structure flip.y
19. Remove top resist - etch photoresist all
20. etch top contact holes
21. Deposit and pattern top Aluminum - deposit aluminum thick=0.5 division=5
22. Deposit top passivation oxide - deposit oxide thick=0.5
23. Etch bond openings
24. flip wafer to p side - structure flip.y

25. p-side(bottom) alumiunum deposition - deposit aluminum thick=0.5 division=5
26. p-side aluminum patterning
27. Deposit P-side passivation oxide - deposit oxide thick=.5
28. P-side passivation oxide etch
29. flip back to top - structure flip.y
30. Sinter and end process

We translate peak doping in the parametrized model into a dose used in ion implantation by integrating the acceptor concentration in the gain layer of the parametrized model. We extract a doping/dose ratio of 6.4×10^{-5}. A peak doping of 3×10^{16} in the previous section nominally corresponds to 1.9×10^{12} implant dose. The ionization integral from the cathode is calculated at each simulation voltage step at specified locations across the device. The simulation stops when the ionization integral exceeds 1 (breakdown), the cathode current exceeds 0.1μAmp or the bias voltage reaches 800V. Devices of 300, 200 and 100 micron thickness are simulated. Electric fields and potentials are probed at 5, 10, 25, 50, 75, 90, 95 percent of the device thickness. We also monitor the impact generation rate in the gain region, which closely parallels the cathode current.

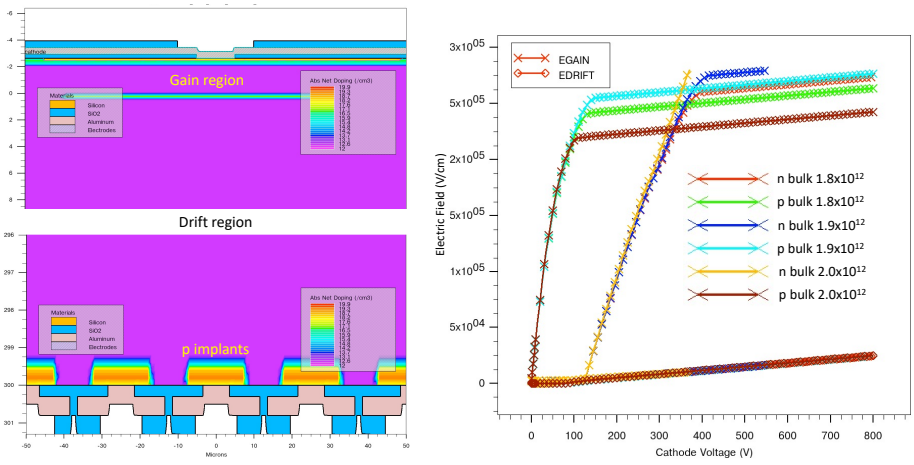

Figure 6: Left) Cross section of top and bottom regions of the double-sided LGAD showing the doping profiles and materials. Note that top and bottom are flipped with respect to the parametric device simulation. Right) Electric field profiles for the gain (crosses) and drift(diamonds) regions of the LGAD.

4.2 Electric Field

Figure 6 shows a profile of the top and bottom regions of the LGAD and the corresponding electric fields as a function of applied bias. Because the p-type

material is depleted from the top the field in the gain region rises immediately until the gain layer is fully depleted at around 125V. At that point the slope of dE/dV is reduced to that characteristic of the full thickness of the LGAD and the drift region starts its depletion. For the n-type material the drift region is depleted first and the gain field only begins to increase when the bulk is fully depleted. The increase in voltage of the gain region is slower then the p-type initial slope. When the gain layer is fully depleted the value of dE/dV is similar to the p-type bulk device.

The bulk field will be limited by the slope of the dE/dV curve in the drift region which is proportional to $1/thickness$. This couples the field in the drift region to the "inflection" voltage where the gain layer is fully depleted. This will tend to limit the drift field to lower values for a thick detector.

4.3 Ionization Integral and Gain

figure 7 shows the ionization integrals and corresponding gains for DS-LGADs with 2.8 micron thickness and gain layer doses of $1.8, 1.9$, and 2.0×10^{12} boron atoms/cm^2. The ionization integral distributions reflect the electric field values in the gain layer. The fast rise in the p-type material as the gain layer is depleted causes a quick rise to moderate ionization integral values. The rate of rise of the ionization integral is moderated when the device is fully depleted and the gain layer field increases more slowly. For the n-type material the ionization integral does not begin to rise until the bulk is fully depleted at about 380 volts. It then rises with a similar slope to the p material until the gain layer is fully depleted when the dII/dV slope is similar to the n material. The *operational range* of the two materials is similar if we require a fully depleted bulk for charge collection however the p type material can be tested for gain at lower voltages.

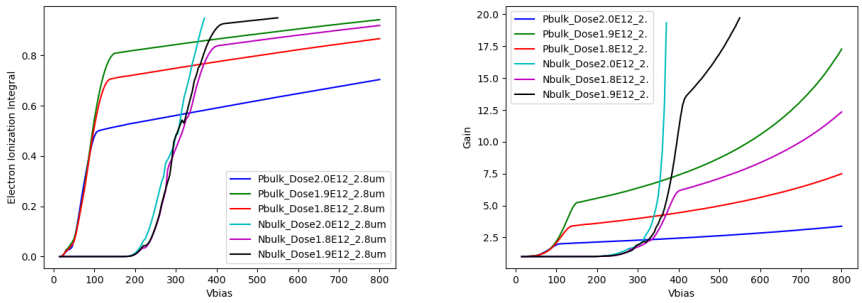

Figure 7: Ionization integral (left) and derived gain values (right) for 300 micron thick double sided LGADs of n and p type bulk with gain layer implant doses of 1.8, 1.9 and 2 $\times 10^{12}$ atoms/cm^2.

The gain is simply defined as $\frac{1}{(1-II)}$ and is shown in figure 7 b. The p-type material starts the fully depleted region at lower values of gain and the gain rises

Type	Thickness μm	slope	intercept	Gain 10	Gain 20	V_{Bias} range	dG/dV gain=20
n bulk	100	5.69E-04	0.762	243	330	88	0.23
p bulk	100	6.52E-04	0.645	391	468	77	0.26
n bulk	200	2.90E-04	0.767	459	631	172	0.12
p bulk	200	3.39E-04	0.667	687	835	147	0.14
n bulk	300	2.02E-04	0.758	703	950	248	0.08
p bulk	300	2.42E-04	0.676	926	1132	207	0.10

Table 1: Operating voltage values for x10 and x20 gain values for 100, 200, and 300 micron thick n and p bulk DS-LGADs.

slowly for these values of gain layer dose. For these parameters the n material can reach useful gain at lower voltage, but as can be seen from the 2.0×10^{12} dose study, it can lead to unstable operation and premature breakdown. For these sets of parameters the best combination would be n bulk with a dose of 1.9×10^{12}.

This choice also depends on the detector thickness as the slope of the post-depletion region is proportional to the device thickness. We have simulated devices with 100, 200 and 300 micron thickness and fit the slope and intercept of the post-depletion ionization integral. We can calculate the voltage needed to operate with a specific gain (in this case 10 and 20) for each set of parameters. The result is shown in table 1.

The last column in Table 1 shows the calculated sensitivity of the gain with respect to voltage at a nominal gain of 20. The lower sensitivity for thicker devices implies more accuracy and control. However the inflection point of the II vs bias curve must be set so that the desired gain can be reached at an acceptably low bias voltage.

5 Conclusions

In these studies we studied the systematics of thick, double sided p and n bulk LGADs. The thickness of the device strongly affects the operating point. This is due to the larger bias needed to deplete the thicker bulk and the smaller $dGain/dV$ slope of thicker sensors. N and p bulk LGADs also have different characteristics due to the opposite directions of bulk depletion. N-type devices must have the bulk depleted before the gain layer begins to deplete. In p-type devices the gain layer begins to deplete almost immediately. These primarily affect the pre-operating point characteristics.

Final doping densities of thick devices must be tuned in parallel with epitaxial thickness and bulk doping density to achieve desired final operation point. The sensitivity of these thick devices to the inflection field implies that thick devices may be more sensitive to the acceptor removal induced by radiation than the usual 50 micron thick bulk sensors.

For initial fabrication studies two hundred micron thick p bulk seems to be a conservative choice. Some gain layer doping process splits should be explored to insure that the operating region is covered.

6 Acknowledgments

This manuscript has been authored by Fermi Research Alliance, LLC under Contract No. DE-AC02-07CH11359 with the U.S. Department of Energy, Office of Science, Office of High Energy Physics.

References

[1] H. F.-W. Sadrozinski, A. Seiden, and N. Cartiglia, "4d tracking with ultra-fast silicon detectors," *Reports on Progress in Physics*, vol. 81, no. 2, p. 026101, 2018.

[2] H.-W. Sadrozinski *et al.*, "Ultra-fast silicon detectors (ufsd)," *Nuclear Instruments and Methods in Physics Research A*, vol. 831, pp. 18 – 23, 2016.

[3] H. F.-W. Sadrozinski *et al.*, "Sensors for ultra-fast silicon detectors," *Nuclear Instruments and Methods in Physics Research A*, vol. 765, pp. 7–11, 2014.

[4] A. Collaboration, "Technical Design Report: A High-Granularity Timing Detector for the ATLAS Phase-II Upgrade," CERN, Geneva, Tech. Rep. CERN-LHCC-2020-007. ATLAS-TDR-031, Jun 2020. [Online]. Available: http://cds.cern.ch/record/2719855

[5] C. Collaboration, "TECHNICAL PROPOSAL FOR A MIP TIMING DETECTOR IN THE CMS EXPERIMENT PHASE 2 UPGRADE," CERN, Geneva, Tech. Rep. CERN-LHCC-2017-027. LHCC-P-009, Dec 2017, this document describes a MIP timing detector for the Phase-2 upgrade of the CMS experiment, in view of HL-LHC running. [Online]. Available: http://cds.cern.ch/record/2296612

[6] N. Cartiglia *et al.*, "LGAD designs for Future Particle Trackers," *Nucl. Instrum. Meth. A*, vol. 979, p. 164383, 2020.

[7] R. Lipton, "A Double Sided LGAD-Based Detector Providing Timing, Position, and Track Angle Information," *FERMILAB-FN-1102-E*, 6 2021.